Struct Chem (2017) 28:1377–1387
DOI 10.1007/s11224-017-0942-y

ORIGINAL RESEARCH

How big are atoms in crystals?

I. David Brown[1]

Received: 14 December 2016 / Accepted: 17 March 2017 / Published online: 8 April 2017

Abstract Atoms and bonds are central concepts in structural chemistry, but neither are concepts that arise naturally from the physics of condensed phases. It is ironic that the internuclear distances in crystals that are readily measured depend on the sizes of atoms, but since atoms in crystals can be defined in many different ways, all of them arbitrary and often incompatible, there is no natural way to express atomic size. I propose a simple coherent picture of Atoms-in-Crystals which combines properties selected from three different physically sound definitions of atoms and bonds. The charge density of the free atom that is used to construct the procrystal is represented by a sphere of constant charge density having the quantum theory of atoms in molecules (QTAIM) bonded radius. The sum of these radii is equal to the bond length that correlates with the bond flux (bond valence) in the flux theory of the bond. The use of this model is illustrated by answering the question: How big are atoms in crystals? The QTAIM bonded radii are shown to be simple functions of two properties, the number of quantum shells in the atomic core and the flux of the bond that links neighbouring atoms. Various radii can be defined. The univalent bonded radius measures the intrinsic size of the atom and is the same for all cations in a given row of the periodic table, but the observed bonded radius depends also on the bond flux that reflects the chemical environment.

Keywords Atom · Bond · QTAIM · Procrystal · Bond flux · Bond valence · Atomic radius · VSEPR model

This paper is dedicated to Professor Lou Massa on the occasion of his Festschrift: A Path through Quantum Crystallography

✉ I. David Brown
idbrown@mcmaster.ca

[1] Brockhouse Institute for Materials Research, McMaster University, Hamilton, ON L8S 4M1, Canada

Introduction

The purpose of this paper is to show that it is possible to define atoms and bonds in a crystal using a model that is easy to manipulate, is physically correct, involves only measurable properties and leads to insights into the factors that determine chemical structure. The Atoms-in-Crystals model is both simple and revealing. It is used to answer the question posed in the title of the paper: How big are atoms in crystals?

The nineteenth century saw the introduction of a model of chemical structure in which atoms are linked by bonds to form molecules. The twentieth century saw the development of quantum mechanics which describes the structure and properties of isolated atoms and molecules, but fails to identify the traditional atoms and bonds that were assumed to form the molecule. The quantum theory of atoms in molecules (QTAIM, [1]) describes a way of dividing the negative charge surrounding the nuclei in a molecule into atomic basins, but the atomic basins do not correspond to the traditional atoms because they do not all contain a nucleus [1 p.42] nor is the network of bond paths that link the basins isomorphous with the network of traditional chemical bonds [2]. Yet, the atom and bond model shows no signs of being abandoned. Both models continue in use because they are complementary and both are needed for a complete description. The atom and bond model are simple and intuitive and can be used to generate plausible molecular and crystal structures using insights that tend to be lost in the quantum mechanical calculations. The atom and bond model are needed to provide the positions of the atoms needed by the Schrödinger equation.

In the original atom and bond model, atoms are assigned a valence equal to the number of bonds the atom can form. In the Lewis model, this valence is identified with valence shell electrons, and each bond is formed by a pair of electrons, one drawn from each of the atoms forming the bond. Bonds of higher order are formed when two or three bonds link the same pair of atoms. The Lewis model assigns one unit of valence to each bond. The model only works well for organic molecules, but it can be extended to inorganic crystals by lifting the restriction that bond orders must be integers. Instead of each unit of valence generating exactly one bond, each atom shares its valence charge in the most symmetric way among as many bonds as it can form, subject to the constraint that the valence of each atom is conserved and that the restrictions of three-dimensional space are respected.

These requirements are built into the bond valence model [3]. In this model, the valence associated with each bond has the same properties as the electrostatic flux, φ, that links the positive charge of the atomic core with the negative charge the atom uses to form the bond. Electrostatic flux, φ, is defined by Eq. 1:

$$\phi = \int \mathbf{E}.d\mathbf{A} \tag{1}$$

where $\boldsymbol{E}$ is the electric field produced by a given charge and the integral is over the area $\boldsymbol{A}$. Integrating Eq. 1 over a complete sphere yields the total flux generated by a charge, V, as shown in Eq. 2:

$$\phi = V/\varepsilon_0 \tag{2}$$

where ε_0 is a dimensional constant. If V is the valence charge of an atom, φ is the total flux that the atom distributes between its various bonds. For convenience, V is measured in electron units, which are also the units of valence, and the constant of proportionality $1/\varepsilon_o$ is chosen as 1.0 so that the bond flux is also measured in valence units, vu. A bond is formed between two atoms when they each contribute a valence charge $-q$ to form the bonding charge of $-2q$. The bonding charge is then linked by a flux, s, to the positively charged cores of each of the two bonded atoms. The flux or valence of a bond, s, is thus equal (in these units) to q, the charge that each atom contributes to form the bond. The important property of the flux is that it depends *only* on the amount of charge contributed to form the bond. Most importantly, it does *not* depend on where the charge is located so that one can imagine the bonding charge to lie either in the middle of the bond, as assumed in the covalent model, or on the anion, as assumed in the ionic model. Whichever model is chosen, the theorems describing the electrostatic flux yield the same result. If the bond network is bipartite, the ionic model is usually preferred, because it allows these theorems to identify stable bond networks and determine the distribution of bond flux [3]. Equation 1 cannot be used directly to determine the bond flux from the quantum mechanical charge distribution because the size and location of the charge used for bonding are not a quantum mechanical observable; hence, its electric field can be neither calculated nor measured, but the bond flux, s, can be determined experimentally because it correlates with the bond length, R, according to either Eqs. 3 or 4 where R_0, B and ν are empirical constants that depend on the bond type [4, 5].

$$s = \exp((R_0 - R)/B) \tag{3}$$

$$s = (R/R_0)^{-\nu} \tag{4}$$

An important property of the flux theory is the *bonding strength*, S, of an atom, which is the flux of a typical bond formed by the atom. It is defined by Eq. 5, where V is the valence of the atom and $<N>$ is its average coordination number:

$$S = V/<N> \tag{5}$$

By convention, the anion is assumed to be oxygen, which is the only anion considered in the present study. The bond network can be constructed by recognizing that stable bonds only form between atoms with similar bonding strengths (the valence matching rule). The distribution of flux among the bonds can be calculated using the two bond network equations. Equation 6 expresses the conservation of bond valence, and Eq. 7 ensures the most symmetric distribution of bond flux [3]:

$$V_i = \sum_j s_{ij} \tag{6}$$

$$0 = \sum_{loop} s_{ij} \tag{7}$$

The subscripts i and j label the bonded atoms. The values of s_{ij} that are the solutions to these equations are the same as the resonance bond numbers derived by Boisson and collaborators for Si-O bonds using the Lewis model [6].

Although the bond flux (i.e., bond valence) provides information about the lengths of the bonds in a crystal (Eqs. 3 or 4), it provides no information about the size of the atoms. The atom size clearly depends on the distribution of negative charge, which for the reasons given above cannot be determined from the bond flux. For an isolated atom (a free atom), the charge distribution is readily calculated, but once the atom is bonded to other atoms, there is no natural way to associate the negative charge with a particular nucleus. QTAIM divides the whole of space into atomic basins or fragments with bond paths linking the charge maxima of basins that share a common face [1]. The intersection of each bond path with its interatomic face is a charge density minimum along the bond path and is known as the bond critical point. The distance

between the charge maximum (normally located at the nucleus) and the bond critical point is known as the *bonded radius* [1]. If the positions of the nuclei are known, all of these properties can be calculated by solving the Schrödinger equation; alternatively, they can be measured by X-ray diffraction.

In general, the interatomic faces in this partitioning are not flat and the bond paths are not straight, but the geometry can be simplified if one replaces the true charge density by the procrystal or promolecule charge density. This is generated by placing the neutral free atom charge densities at the locations of their corresponding nuclei in the crystal. The result is a surprisingly good approximation to the true charge density [7]. While the difference, known as the deformation density, is significant, it is small and rarely exceeds 1 e.Å^{-3}.

The topologies (the arrangements of basins and bond paths) of the true and procrystal charge distributions are identical, and their geometries (the locations of the bond critical points) differ by only a few hundredths of an Ångström [7]. The principal difference between the QTAIM and procrystal descriptions lies in the way in which the atoms are defined. In the QTAIM partitioning, the atoms are space filling fragments with clearly defined boundaries separating the atoms, and while the procrystal density can also be partitioned in this way, it is more convenient to define atoms by the free atom charge densities used to construct the procrystal. The result is a picture of overlapping spherical atoms. This definition of an atom has many advantages. Every atom of a given element has exactly the same charge density regardless of its valence state or bonding environment. All the atoms are spherically symmetric and electrically neutral and remain so however they are manipulated. Since the procrystal charge density is obtained by adding together the charge densities of the atoms, moving the atoms changes the procrystal charge density while preserving the charge densities of the individual neutral atoms. The procrystal charge density is readily calculated from the known free atom charge densities, though for many applications, a numerical value is not needed. Finally, the difference between the procrystal and true charge densities, i.e., the deformation density, is readily calculated, allowing its physical significance to be assessed.

The adoption of a picture of neutral atoms does not invalidate the use of the ionic model. The charge that actually forms the bond presumably lies in the region where the atoms overlap, but since the bond flux does not depend on knowing the physical location of this charge, the electrostatic flux theorems can be used even when the bonding charge is assumed to lie entirely on the anion. Assigning a formal charge to each atom does not imply a physical charge transfer, and the true charge density is always correctly approximated by the neutral atoms of the procrystal.

This study uses a model that combines these ideas. Atoms-in-Crystals takes features from each of the above models. The atoms are defined as the neutral free atoms of the procrystal model and are represented by a spherical contour of constant charge density. The radius of this sphere is the QTAIM bonded radius thus ensuring that the spheres representing two bonded atoms just touch at the bond critical point. Each bond in this network is characterized by its electrostatic flux which is equal to the charge (valence) contributed by each of the two bonded atoms. Since the bond is usually straight in this model, its length is assumed to be equal to the sum of its two bonded radii. Atoms whose bonds are not all the same length are represented by several concentric spheres, each corresponding to one of the bond lengths.

Bond lengths

In the early days of the ionic model, atoms were assumed to be spheres having radii that were characteristic of the ion. The radii could be calculated from the lengths of the bonds, but only if the absolute radius of one atom was already known, which in practice meant that the radius of oxygen had to be arbitrarily chosen. Different choices led to different scales which have been well reviewed by Gibbs and colleagues [8]. As the structures of more complex crystals were published, it was realized that the radius of an atom also depends on its coordination number, leading to the Shannon-Prewitt list of atomic radii which define the bond type not only by the chemical element and its valence but also by its coordination number [9]. While this improved the accuracy with which radii could be used to predict average bond lengths, it did not account for the variable lengths of the individual bonds formed within the same coordination sphere.

Gibbs and collaborators [10] have used quantum methods to calculate M-O bond lengths, R_{MO}, in symmetric coordination spheres with different coordination numbers, N, for a variety of cations, M, to show that in these systems, the relationship between bond length and the Pauling bond strength, $<s>$, is given by Eq. 8.

$$R_{MO} = 1.39(< s > /n)^{-0.22} \tag{8}$$

Here, n is the row number of the cation in the periodic table (ignoring the row with hydrogen and helium), and the Pauling bond strength, defined in Eq. 9, is the average flux of the bonds formed by an atom with a coordination number N.

$$< s >= V/N \tag{9}$$

As the row number, n, is equal to the number of quantum shells in the atomic core, it can serve as a measure of the

intrinsic size of an atom. Equation 8 can be rewritten as Eq. 10 (c.f. Eq. 4).

$$< s >= n[1.39/R_{MO}]^{4.55} \quad (10)$$

Since the bond - flux - bond - length relation can be equally well represented by either the exponential function (Eq. 3) or the power law (Eq. 4), it is reasonable to expect that Eq. 10 could, with a suitable choice of parameters, equally well describe the relationship between the flux, s, and the length, R_{MO}, of an individual M-O bond using Eq. 11.

$$s = n \times \exp((R_0 - R_{MO})/b) \quad (11)$$

Equation 11 can be rewritten in the form of Eq. 12:

$$R_{MO} = R_1 - B_1 \ln(s/n) \quad (12)$$

which can be expanded to give Eq. 13:

$$R_{MO} = R_1 + B_1 \ln(n) - B_1 \ln(s) \quad (13)$$

This equation is both physically revealing and easily tested. Using the two fitted parameters (R_1, B_1) = (1.38, 0.36) Å, the calculated values of R_{MO} reproduce the observed M-O bond lengths for Main Group cations, M, with an accuracy of about 0.1 Å. Although not accurate enough for quantitative work, Eq. 13 shows that the sizes of atoms, as represented by their bond lengths to oxygen, follow a remarkably simple pattern that reveals much about the physics of the chemical bond. The length of an M-O bond depends primarily on just two parameters: n, being the core size of the cation M, representing the repulsive force tending to lengthen the bond, and s, the bond flux, representing the attractive force tending to shorten the bond. The repulsive term depends on the intrinsic size of the atoms; the chemistry is all contained in the attractive term that depends on the way the bonding charge relaxes when the crystal is formed.

Equation 13 can be simplified by replacing the first two terms by R_n

$$R_{MO} = R_n - B_1 \ln(s) \quad (14)$$

where

$$R_n = R_1 - B_1 \ln(n) \quad (15)$$

When $s = 1$, R_{MO} and R_n are equal, showing that R_n, which is the length of a univalent M-O bond, depends only on the size of the atomic core; Eq. 15 also implies that all the cations in the same row of the periodic table should have the same univalent M-O bond length, and presumably the same univalent radius.

Not many Main Group cations actually form univalent bonds; the fluxes observed for most M-O bonds are either much larger or much smaller than 1.0 vu. A more typical M-O bond is one that has a bond flux equal to the cation bonding strength, S, given by Eq. 5. The length of such a bond, R_S, known as the *typical bond length*, is the length of the bond most likely to be found in a crystal. Substituting the bonding strength, S, for the flux, s, in Eq. 13 gives Eq. 16 which defines the typical length, R_S, of an M-O bond. Most of the following discussion focuses on the typical bond.

$$R_S = R_1 + B_1 \ln(n) - B_1 \ln(S) \quad (16)$$

The flux, s, shown in Eq. 13 can be decomposed into two parts as shown in Eq. 17.

$$s = S + \Delta s \quad (17)$$

S is the bonding strength of the cation that determines the typical bond length. It is an intrinsic property of the atom related to its position in the periodic table. Δs is the change in the bond flux that occurs when the bond network relaxes to its equilibrium state. The value of s, hence Δs, is determined by the network equations (Eqs. 6 and 7) the latter being the condition that leads to the most symmetric distribution of fluxes among the bonds.

Atomic radii

In order to extend this analysis from bond lengths to bonded radii, a set of measured bonded radii is needed. Gibbs and collaborators [8] have reported bonded radii, r_M, and r_O, for 14 Main Group M-O bond types in various high symmetry MO_N configurations. Since all the bonds in each of the given configurations are the same length, their bond fluxes are equal to the Pauling bond strength (Eq. 9), and the bonded radii of the atoms are all measured using the calculated true charge-density distribution. Among the bond types they report are MgO_N polyhedra with the four different coordination numbers, N, shown in Table 1. The bond fluxes, s_{MgO}, are listed in column 2, the bond lengths, R_{MgO}, in column 3, and the bonded radii, r_{Mg} and r_O, in columns 4 and 5.

As expected, the radii of both the magnesium and the oxygen atoms increase as the bond length increases and the bond flux decreases, but the *fractional bonded radii*, f_{Mg} and f_O,

Table 1 Variation in the bond radii, r, and fractional bonded radii, f, of Mg^{2+} and O^{2-} with bond flux, s, and bond length, R

	s_{MgO} (vu)	R_{MgO} (Å)	r_{Mg} (Å)	r_O (Å)	f_{Mg} Eq. 18	f_O Eq. 19
MgO_4	0.50	1.91	0.84	1.07	0.44	0.56
MgO_5	0.40	2.07	0.90	1.17	0.43	0.57
MgO_6	0.33	2.14	0.94	1.20	0.44	0.56
MgO_8	0.25	2.27	0.96	1.31	0.42	0.58

Values of the bonded radii, r_M and r_O, are taken from [8]. The bond fluxes, s_{MgO}, are calculated from Eq. 9

defined in Eqs. 18 and 19 and listed in the last two columns, are independent of the bond flux.

$$f_M = r_M/R_{MO} \tag{18}$$

$$f_O = r_O/R_{MO} \tag{19}$$

For Mg-O bonds, the fractional bonded radii, $f_{Mg} = 0.43$ and $f_O = 0.57$, are invariant and do not depend on the bond flux or bond length so that f_M and f_O can be calculated if the bonded radii are known for just one bond. The fractional bonded radii can then be used to calculate r_M and r_O for any other Mg-O bond whose length, R_{MO}, is known. As Gibbs and collaborators point out, and as the constancy of the fractional bonded radii show, increasing the length of a bond increases both the cation and the anion bonded radii in fixed proportions [8]. The anion radius is not a constant as assumed in many atomic radius models (see the discussion in [8]).

Table 2 lists the bonded radii, r_M and r_O (columns 4 and 5), and fractional bonded radii, f_M and f_O (columns 6 and 7), of the 14 M-O bond types reported by Gibbs and collaborators [8]. Although they report some of these radii for MO_N complexes with more than one coordination number, N, the radii shown in Table 2 are the *typical bonded radii* corresponding to the cation bonding strengths shown in column 2. Some values have been interpolated between the values given in reference [8].

According to Eq. 15, the univalent bond lengths are expected to be the same for all elements in the same row of the periodic table, and one might therefore expect the fractional bonded radii to be equal as well. This is seen to be at least approximated true if one ignores the highly anomalous nitrogen and oxygen. The deviations are small but appear to be systematic, and while they are worthy of further study, they are ignored in this analysis. The best values of the fractional bonded radii for each row, n, of the periodic table are shown in columns 2 and 3 of Table 3, though for consistency with later analysis, the values listed are derived from Table 4 rather than Table 2.

Table 2 Typical and fractional radii of cation bonds to oxygen

	S_M (vu)	R_S (Å)	r_M (Å)	r_O (Å)	f_M	f_O
^{6}Li	0.20	2.21	0.82	1.39	0.37	0.63
^{4}Be	0.50	1.65	0.58	1.07	0.35	0.65
$^{3.5}B$	0.87	1.43	0.48	0.95	0.34	0.66
^{3}C	1.33	1.29	0.46	0.83	0.36	0.64
^{3}N	1.67	1.24	0.60	0.64	0.48	0.52
^{1}O[a]	2.00	1.15	0.58	0.58	0.50	0.50
^{6}Na	0.16	2.44	1.09	1.35	0.45	0.55
^{6}Mg	0.33	2.14	0.94	1.20	0.44	0.56
^{5}Al	0.57	1.86	0.78	1.08	0.42	0.58
^{4}Si	1.00	1.62	0.67	0.95	0.41	0.59
^{4}P	1.25	1.54	0.63	0.91	0.41	0.59
^{4}S	1.50	1.47	0.58	0.89	0.39	0.61
^{6}K	0.13	2.87	1.44[b]	1.43[b]	0.50	0.50
^{8}Ca	0.27	2.52	1.25	1.27	0.50	0.50
Transition metals[c]					0.50	0.50
^{4}Ge	0.89	1.74	0.83	0.91	0.48	0.52

Bonding strengths, S_M, are taken from [3]. Bonded radii, r, and bond lengths, R, are taken from [8]. Fractional radii, f, are calculated using Eqs. 18 and 19 from values given in the table

[a] Determined from the observed O-O distance in O_2. This value is not reported in [8]. It is not strictly comparable to the other values given since it applies to the O^{2+}-O^{2-} bond, not the O^{6+}-O^{2-} bond

[b] Estimated. Reference [8] only gives radii for a bond flux of 0.17 vu

[c] The transition metals reported in [8] are divalent Mn, Fe and Co.

Table 5 Definition of columns

1. Element
2. S taken from Table 2.1 of reference [3] calculated using Eq. 5 with $<N_O>$
3. S from Eq. 5 using $<N>$ in column 14
4. R_0 bond valence parameter from [5]
5. r_{SM} calculated from Eq. 21
6. r_{SM} calculated from column 9 minus column 7
7. r_{SO} calculated from Eq. 22 with radius valence parameters (0.93, 0.25) Å
8. R_S calculated using Eq. 25 with S in column 2
9. R_S calculated from Eq. 3 using parameters (R_0, 0.37) Å with the R_0 given in column 4 and S in column 2
10. R_S taken from [8] and shown in Table 2
11. f_M calculated by subtracting column 12 from 1.0
12. f_O calculated from Eq. 19 with values of r_{SO} in column 7
13. f_O taken from Table 2
14. $<N>$ calculated from r_M using Eq. 27
15. $<N_O>$ average coordination numbers in observed structures taken from Table 2.1 of reference [3, 12]

Following Eq. 14, the typical bonded radii, r_{si}, of the atoms i in each row of the periodic table shown in Tables 2 can be

Table 3 Best values of the fractional, f, and univalent bonded radii, r_0, and the corresponding bond length, R_n, for univalent M-O bonds for M in different rows, n, of the periodic table

n Row	f_M	f_O	r_{0M} Å (s = 1 vu)	r_{0O} Å (s = 1 vu)	R_n Å $r_{0M} + r_{0O}$	R_0[a] Å [11]	R_n Å Eq. 15
1	0.33	0.67	0.47	0.93	1.40	1.38	1.38
2	0.43	0.57	0.72	0.93	1.65	1.62	1.63
3	0.49	0.51	0.83	0.93	1.76	1.80[b]	1.76
4	0.51	0.49	0.99	(0.93)	1.92		1.88
5	0.53	0.47	1.09	(0.93)	2.02		1.96

The fraction radii, f, are obtained by averaging those shown in Table 4. The univalent bonded radii, r_0, are taken from Table 5 (method 2) Values in parenthesis are assumed

[a] Values of R_0 for bonds by cation row are taken from Table 2 of reference [11]

[b] Fitted to the cations from K^+ to Cr^{6+} and so not strictly comparable with the other values or R_n

Table 4 Bonding strengths, S, typical bonded radii, r_S, typical bond lengths, R_S, fractional bonded radii, f, and typical coordination numbers <N> for main group elements determined in different ways

Element	S vu Eq. 5	S vu Eq. 28	R_0 Å	r_{SM} Å Eq. 21	r_{SM} Å Eq. 23	r_{SO} Å Eq. 22	R_S Å Eq. 25	R_S Å Eq. 3	R_S Å [8]	f_M 1-f_O	f_O Eqs. 19 and 22	f_O Table 2	<N_{calc}> Eq. 17	<N_O> [12]
Li	0.20	0.18	1.466	0.695	0.729	1.332	2.008	2.061	2.21	0.35	0.65	0.63	5.50	4.90
Be	0.50	0.48	1.381	0.567	0.534	1.103	1.650	1.637	1.65	0.33	0.67	0.65	4.37	3.99
B	0.87	0.79	1.371	0.489	0.458	0.965	1.434	1.423	1.43	0.32	0.68	0.66	3.80	3.46
C	1.35	1.17	1.390	0.430	0.426	0.859	1.269	1.284	1.29	0.33	0.67	0.64	3.43	2.96
N	1.67	1.51	1.432	0.398	0.440	0.802	1.242	1.242	1.24	0.35	0.65	0.52	3.32	3.00
Na	0.16	0.15	1.803	1.068	1.093	1.388	2.346	2.481	2.44	0.44	0.56	0.55	6.62	6.40
Mg	0.33	0.36	1.693	0.930	0.896	1.207	2.117	2.103	2.14	0.43	0.57	0.56	5.62	5.98
Al	0.57	0.60	1.651	0.826	0.788	1.071	1.877	1.859	1.86	0.42	0.58	0.58	4.96	5.27
Si	1.00	0.92	1.630	0.720	0.700	0.930	1.630	1.630	1.62	0.43	0.57	0.59	4.35	4.02
P	1.25	1.22	1.617	0.677	0.660	0.874	1.531	1.534	1.54	0.43	0.57	0.59	4.10	4.01
S	1.50	1.52	1.624	0.642	0.645	0.829	1.451	1.474	1.47	0.44	0.56	0.61	3.94	4.00
Cl	1.75	1.84	1.632	0.613	0.635	0.790	1.383	1.425		0.45	0.55		3.80	4.00
K	0.13	0.13	2.132	1.355	1.447	1.440	2.775	2.887	2.87	0.50	0.50	0.50	7.71	7.90
Ca	0.27	0.31	1.967	1.180	1.194	1.257	2.417	2.451	2.52	0.49	0.51	0.50	6.54	7.31
Ga	0.65	0.60	1.730	0.969	0.852	1.038	1.987	1.889		0.45	0.55		5.04	4.62
Ge	0.89	0.84	1.748	0.893	0.832	0.959	1.833	1.791	1.74	0.46	0.54	0.52	4.78	4.51
As	1.13	1.09	1.767	0.836	0.822	0.899	1.716	1.722		0.48	0.52		4.60.	4.41
Se	1.50	1.33	1.788	0.803	0.827	0.864	1.647	1.691		0.49	0.51		4.52	4.00
Br	1.5	1.58	1.810	0.768	0.831	0.829	1.577	1.660		0.50	0.50		4.43	4.00
Rb	0.12	0.12	2.263	1.510	1.583	1.450	2.940	3.032		0.52	0.48		8.10	8.00
Sr	0.23	0.28	2.118	1.347	1.363	1.294	2.621	2.656		0.51	0.49		7.09	8.57
In	0.50	0.52	1.902	1.148	1.055	1.102	2.231	2.157		0.49	0.51		5.76	5.98
Sn	0.68	0.73	1.905	1.068	1.021	1.025	2.074	2.046		0.50	0.50		5.64	5.86
Sb	0.83	0.94	1.912	1.019	1.005	0.978	1.976	1.983		0.51	0.49		5.29	6.05
Te	1.00	1.17	1.917	0.969	0.987	0.930	1.879	1.917		0.52	0.48		5.18	6.00
I	1.32	1.38	2.003	0.897	1.040	8.600	1.737	1.900		0.55	0.45		5.07	5.30
Cs	0.11	0.12	2.417	1.712	1.752	1.482	3.173	3.234		0.54	0.46		8.63	9.20
Ba	0.20	0.26	2.285	1.532	1.548	1.332	2.845	2.880		0.54	0.46		7.69	10.21
Tl	0.49	0.50	2.003	1.263	1.159	1.108	2.352	2.267		0.51	0.49		6.05	6.40
Pb	0.70	0.69	2.042	1.156	1.155	1.019	2.156	2.174		0.53	0.47		5.80	5.73
Bi	0.8	0.87	2.060	1.116	1.157	0.986	2.082	2.143		0.54	0.46		5.72	6.00

Table 5 Parameters used in Eq. 20

	r_{0M} (Å) Eq. 20	r_{0M} (Å) Eq. 21	b_M (Å) Eq. 20	r_{0O} (Å) Eq. 20	b_O (Å) Eq. 20	B_n= $b_M + b_O$
First row (1)[a]	0.48		0.20	0.91	0.26	0.46
First row (2)[a]	0.47	0.47	0.14	0.93	0.28	0.42
Second row (1)	0.67		0.25	0.97	0.21	0.45
Second row (2)	0.72	0.73	0.19	0.93	0.25	0.44
Third row (1)[b]	0.83		0.33	0.89	0.30	0.63
Third row (2)	0.83	0.88	0.24	(0.93)	(0.25)	0.49
Fourth row (2)	0.99	0.97	0.26	(0.93)	(0.25)	0.51
Fifth row (2)	1.09	1.06	0.30	(0.93)	(0.25)	0.55

Values in parentheses are assumed

(1) means fitted to all the bonded radii and distances reported in [8]. (2) means fitted to bonded radii equal to $f \times R_S$ with f given in Table 3 and R_S calculated using Eq. 3

[a] Excluding nitrogen and oxygen

[b] These values are less reliable as reference [8] provides no radii for high valence cations

reproduced using Eq. 20 with the parameters (r_{0i},b_i) shown in Table 5.

$$r_{Si} = r_{0i} - b_i \ln(S) \tag{20}$$

where S is the cation bonding strength.

The parameters for Eq. 20 shown in Table 5 are calculated in two different ways. Those labelled (1) were fitted against all the bonded radii reported in [8], some of which are shown in Table 2. Those labelled (2) were fitted against the radii calculated by multiplying R_S in column 8 of Table 4 by the values of f in Table 3. The difference between these two sets of parameters is not significant, except for the values of b_M which reflect the different estimates of the values of R_S. Excluding the cations nitrogen and oxygen, the parameters (r_{0i},b_i) in Table 5 reproduce the radii from which they were derived with a root mean square deviation of less than 0.02 Å.

The values of r_{0M} and r_{0O} in Table 5 are the *univalent bonded radii* of the cations and anions, respectively. They are an invariant measure of atom size that does not depend on the nature of the bonds that they form.

By analogy with Eq. 16, Eq. 20 can be expanded to include both the terms n and S.

$$r_{SM} = r_{1M} + b_{nM} \ln(n) - b_{nM} \ln(S) \tag{21}$$

The typical bonded radius of any cation is given by Eq. 21 using the fitted parameters (r_{1M},b_{nM}) = (0.47,0.36) Å. These radii are shown in column 5 of Table 4. Equation 21 shows that the typical bonded radii, like the typical bond lengths, depend only on n and S. They are therefore characteristic properties of an atom that can be determined without reference to the charge density distribution, further justifying the use of bonded radii as an appropriate measure of the size of an atom in a crystal.

In the earlier scales of atomic radii, the radius of oxygen was assumed to be a constant, but in their study of bonded radii, Gibbs and collaborators [8] illustrated that this was not so; the radius of oxygen increases in the same proportion as the radius of the cation as the bond length increases, as shown by the constancy of the fractional radii, f, for all the bonds of the same type. The typical bonded radius of oxygen therefore depends, not as one might have expected, on the coordination number of the oxygen atom, but rather on the typical bonded radius of the cation; hence, it depends on the typical coordination number, $<N>$ of the cation. The reason for this unexpected result is discussed below, but the consequence is that the typical bonded radius of oxygen is different for every bond type and can only be determined once the cation is known. The relationship between the typical bonded radius of oxygen, r_{SO}, and the bonding strength of the cation, S_M, is illustrated in Fig. 1 and given by Eq. 22.

$$r_{SO} = r_{0O} - b_O \ln(S_M) \tag{22}$$

with (r_{0O},b_O) = (0.93,0.25) Å taken from Table 5.

Since the fitted parameters of Eq. 22 are independent of the choice of the cation, subtracting the oxygen bonded radius of Eq. 22 from the typical bond length, R_S, provides an alternative method of calculating the typical bonded cation radius as shown in Eqs. 23 and 24.

$$r_{SM} = R_S - r_{SO} = (R_0 - B\ln(S)) - (r_{0O} - b_O \ln(S)) \tag{23}$$

hence

$$r_{SM} = (R_0 - r_{0O}) - (B - b_O)\ln(S) = r_{0M} - b_M \ln(S) \tag{24}$$

where $R_0 = r_{0M} + r_{0O}$ and $B = b_M + b_O$.

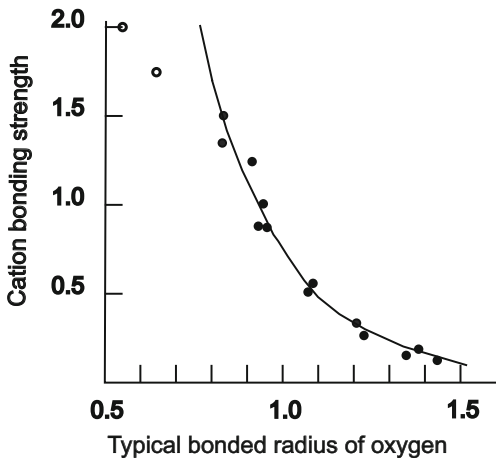

Fig. 1 The relationship between the bonding strength of the cation and the typical bonded radius of the oxygen atom. The points are the radii reported in [8]. The *open circles* are nitrogen and oxygen (see Table 2). The *line* is calculated using Eq. 22 with the parameters (r_{0O},b_O) = (0.93,0.25) Å

Table 4 brings together all the properties of the Main Group cations, some calculated in more than one way. The bonding strengths, S, for the Main Group cations in their highest oxidation state are listed in column 2 [3]. These are used to calculate the typical M-O bond lengths, R_S, (column 9) using Eq. 3 with bond valence parameters (R_0,0.37) Å, where R_0 is given in column 4. Equation 22 was used to calculate the corresponding bonded radius of oxygen, r_O, (column 7). The difference between R_S (column 9) and r_{SO} (column 7) calculated with Eq. 23 is the typical bonded radius of the cation, r_{SM}, shown in column 6. The root mean square difference between the values of r_{SM} calculated using Eq. 21 (column 5) and those calculated using Eq. 23 (column 6) is 0.05 Å. If one excludes nitrogen, the same difference is found between the cation radii shown in columns 5 and 6 and the radii measured from the calculated charge densities reported in [8] and shown in column 4 of Table 2.

The fractional bonded radii of oxygen, f_O, shown in column 12 are obtained from the typical bonded radii, r_{SO}, calculated using Eq. 22. The values of f_M shown in column 11 are calculated by subtracting f_O from 1.0. These values were used to calculate the fractional bonded radii shown in Table 3. The root mean square difference between the fractional bonded radii of oxygen, f_O, derived from the bonded radii reported in [8] (column 13) and those calculated using Eq. 19 (column 12) is 0.02 if nitrogen is excluded.

The univalent cation bonded radii, r_{0M}, for each row in the periodic table are shown in Table 5. The radii in column 3, calculated by setting S = 1.0 vu in Eq. 21, are in satisfactory agreement with those in column 2 calculated using Eq. 20.

There is no reason why both the prelogarithmic parameters, B_1, in Eq. 13 should be the same. Equation 24 suggests that a better parameter, B_n, is given by the sum $b_M + b_O$ shown in the last column of Table 5. By substituting this value in Eq. 13, one gets Eq. 25:

$$R_S = R_1 + B_1 \ln(n) - B_n \ln(S) \tag{25}$$

where, as before, (R_1,B_1) = (1.38,0.36) Å and the values of B_n are taken from the last column of Table 5 (method 2). The values of R_S calculated this way are shown in column 8 of Table 4. The difference between values of R_S calculated using Eq. 25 (column 8) and those calculated using Eq. 3 (column 9) is 0.07 Å, where much of the variation can be attributed to a systematic tendency of Eq. 25 to underestimate R_S by about 0.05 Å for cations in Groups 1 and 17, and overestimate it for cations close to Group 13 by a similar amount. As mentioned above, exploring the origin of this deviation is beyond the scope of this paper.

Alternatively, Eq. 25 can be written as

$$R_S = R_n - B_n \ln(S) \tag{26}$$

whereas before R_n is the univalent bond length equal to $r_{0M} + r_{0O}$ shown in column 6 of Table 3. Earlier, Shannon and I showed empirically that Eq. 4 could be used with a single set of parameters (R_0,ν) to calculated the M-O bond strengths (i.e., bond fluxes) for all the Main Group cations in the same row of the periodic table [11]. The values of R_0 we reported at that time are the univalent bond lengths shown in column 7 of Table 3. The univalent radii calculated using Eq. 15 with (R_1,B_1) = (1.38,0.36) Å are shown in column 8. The three different determinations of R_n agree within 0.03 Å.

A key concept in the bond flux model is the bonding strength of an atom which describes the flux expected for a typical bond as defined in Eq. 5. There should therefore be a direct relationship between the typical coordination number $<N_O>$ and the typical bonded radius, r_{SM}. The values of $<N_O>$ shown in the last column of Table 4 are averages of the coordination numbers of MO_N groups in an early unpublished version of the Inorganic Crystal Structure Database (ICSD) [12, 13]. In spite of the inherent biases in this sample, the bonding strengths derived using these values of $<N_O>$ have proved to be robust. There is a correlation between $<N_O>$ and r_{SM}, but a simpler correlation is found between $<N_O>$ and the typical bond length, R_S (Eq. 27):

$$< N_{calc} > = k' R_S \tag{27}$$

where k' = 2.67 Å^{-1} and the values of R_S are those calculated using Eq. 3. The typical coordination number $<N_{calc}>$ predicted by Eq. 27 is shown in the second to last column of Table 4. With a few exceptions, the observed and calculated values of the typical coordination number differ by less than 0.5. The calculated values are systematically higher than those observed for the first row, particularly for lithium. The large calculated values for carbon and nitrogen may well be better estimates than the observed average of 3.00 since the average is a poor estimate of the ideal coordination number when the cation is known with only one coordination number. This problem also affects the cations in Groups 16 and 17. The exploitation of the unusual properties of perovskites resulted in the early versions of the Inorganic Crystal Structure Database containing many reports of barium coordination number 12, which accounts for the high observed value of $<N_O>$ for barium (10.21 against the calculated value of 7.69). The distribution of barium coordination numbers for oxygen ligands has a mode at 9 and a spike at 12. If the structures with N = 12 are omitted (many are likely misassigned and others stabilized only by high temperatures and by the high symmetry of the perovskite structure), the average coordination number drops to 8.33, which is close to the mode and the value predicted by Eq. 27.

Combining Eq. 27 with Eqs. 5 and 25 gives Eq. 28 which shows that the calculated value $<N_{calc}>$ is not independent of

the assumed value of $<N_O>$, but since the value $<N_O>$ appears in a relatively small correction term, any error in $<N_O>$ results in an error in $<N_{calc}>$ that is ten times smaller.

$$< N_{calc} > = \acute{k} (R_1 + B_1 \ln(n) - B_n \ln(V / < N_O >)) \quad (28)$$

Equation 5 can be used to convert the values of $<N_{calc}>$ (Eq. 27) to the values of S shown in column 3 of Table 4. The root mean square difference between the two values of S in columns 2 and 3 is 0.04 vu which is a little larger than the estimated uncertainties in either value.

Oxygen, lone pairs and the VSEPR model.

Implicit in this analysis of the size of atoms in crystals is the asymmetry between the bonding properties of cations and anions; most notably, the typical bonded radii of both the cation and the anion are determined by the bonding strength of the cation. The valence matching rule mentioned in the 'Introduction' states that a bond will only form between atoms whose bonding strengths differ by less than a factor of two [3]. Assuming an average coordination number of four, oxygen has a bonding strength of 0.50 vu and so should only form bonds to cations with bonding strengths between 0.25 and 1.00 vu, but the bonding strengths of cations in Groups 15 to 17 are much larger; for example, Cl^{7+}, which is found in ClO_4^-, has a bonding strength of 1.75 vu. The ability of oxygen to form bonds stronger than 1.00 vu arises from the presence of nonbonding 'lone-pair' charge in its valence shell. According to the octet rule, anions have more charge in their valence shells than they can use for bonding. When an anion forms many weak bonds, the bonding and nonbonding charge is uniformly distributed around its spherical valence shell, but when the anion is required to bond to cations with large bonding strengths, it uses most of its bonding charge to form strong primary bonds, leaving any residual bonding charge able to form only weak secondary bonds. In order to maintain a spherical valence shell, the nonbonding lone pairs must be moved into the region occupied by the secondary bonds. Bickmore and collaborators [14] have shown that when the bonding strength of the cation exceeds the bonding strength of oxygen (0.50 vu), the lone pairs become stereoactive with the degree of stereoactivity increasing as the bonding strength of the primary cation increases.

This picture mirrors the Valence Shell Electron Pair Repulsion (VSEPR) model of Gillespie and collaborators [15, 16] with the electron pairs of the VSEPR model replaced by the flux that links them to the atom core. The bonding strength of the primary cation determines the flux, hence the length, of the primary bonds, and the extent of the stereoactivity of the lone pair. Any remaining valence determines the flux available to form the secondary bonds. The rules of the VSEPR model determine how the primary bonds and lone pairs are arranged within the spherical valence shell and indicate the angles between the bonds. The Atom-in-Crystals model displays atoms with lone pairs that simultaneously form both primary and secondary bonds by using several concentric spheres, one for each of the different bond lengths. For example, the oxygen atoms in Na_2SO_4 would be displayed by two or more spheres, one having a bonded radius of 0.83 Å representing the flux of 1.50 vu that forms the primary bond to sulphur, and one or more spheres having a bonded radius of ~1.37 Å representing the flux of ~0.17 vu used to form bonds to two or three sodium atoms as shown in Fig. 2.

Discussion

Atoms-in-Crystals is a model in which a procrystal is constructed from the charge densities of the neutral free atoms. These atoms can be visualized by one or more spherical contours of constant charge density, each having a radius equal to one of the bonded radii of the QTAIM partitioning of the true charge density. The atoms are linked by bonds whose electrostatic bond flux is equal to the amount of valence charge contributed by each atom. The charge density of this model closely follows the true charge density, and while the difference between the procrystal and true density is significant, it is small; it can readily be assessed from the deformation density. The purpose of this paper has been to show that the atoms of this model have a natural bonded radius that can be determined in two ways, either from a QTAIM partitioning of the

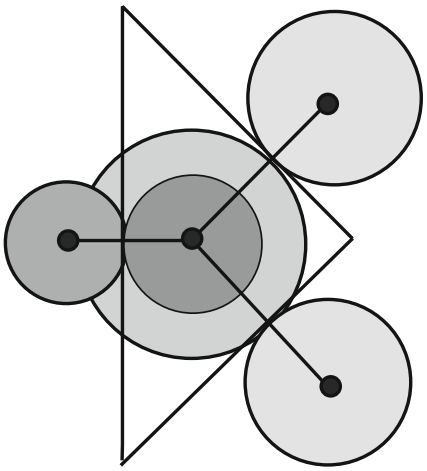

Fig. 2 The depiction of an asymmetrically bonded anion in the Atoms-in-Crystals picture. The procrystal atoms are shown as *shaded circles*, where the *dark circles* are contours of higher charge density and bond flux. The central anion is represented by two *concentric circles* whose inner and outer radii correspond to the primary and secondary bonds, the QTAIM topology is shown by the *straight lines*. The *spheres* touch at the bond critical points and their *tangents* show where the bonding surfaces of the QTAIM anion intersect the plane of the figure

charge density or from an Atoms-in-Crystals analysis of the core sizes of the atoms and the network of the bonds.

While the model describes chemical structure using the concepts of the traditional atom and bond model, it also provides a close approximation to the true physical charge density. As shown elsewhere [3], it can be used for quantitative predictions of both the topology and geometry of chemical structures and their related properties, using little more computing power than is provided by a pocket calculator. Its description of the charge density is sufficiently accurate to allow it to be used for qualitative analysis. For example, when two atoms with nearly full valence shells form a bond, such as that in the F_2 molecule, the Atoms-in-Crystals model places more charge in the bonding region than it can accommodate. Some charge must be moved into the unoccupied space of the valence shells in the regions of the lone-pairs. This polarization is seen in the deformation density as negative charge transferred from the bond to the empty portion of the nonbonding region of the valence shell. The amount of charge transferred is small, but it has a large effect on the bond energy; the electrostatic bond energy is reduced from 133×10^{-3} a.u. in the procrystal to 6×10^{-3} au in the real crystal [17], an effect that puzzled Sanderson [18] who called it the 'lone pair weakening effect'.

The model is not offered as a replacement for the full quantum theory of chemical bonding, but rather as a simpler and more intuitive complement. It presents an alternative way of decomposing the charge density into atomic fragments. The Atoms-in-Crystals description of the charge density is an approximation, but what is lost in this approximation is more than compensated for by the simplicity of the model: All atoms of a given element have the same simple geometry, and all are, by definition, electrically neutral and unaffected by changes in their environment. This makes it easy to visualize the changes that occur in the charge density when the bond lengths are altered by changing, for example, the oxidation states (valences) of the atoms. Unlike the atomic basins and bond paths of QTAIM, the atoms and bonds of the Atoms-in-Crystals model have the same properties as the traditional atoms and bonds of structural chemistry, thus providing the familiar empirical terms with a physical description.

Atoms-in-Crystals is a simple model that is accessible to anyone with a secondary school science education, and because the model is based on a qualitatively correct picture of the charge density, it can be developed into a proper quantum mechanical description later in the undergraduate curriculum. It also has many features that make it ideal for exploring the physics of chemical bonding. For those who like to interpret chemical structures in terms of atoms and bonds, it provides atoms that are always rigid and electrically neutral, and bonding relationships determined by classical electrostatics. The properties of the bond flux show that the ionic model is a legitimate mathematical fiction which can be used to develop theorems that confirm and extend the rules of the more successful empirical models, such as the ionic and VSEPR models, while revealing the limitations of models that use concepts that have no basis in physics, such as electron orbitals and Lewis electron pairs.

Glossary

V	Atomic valence	The amount of charge in *valence units* (electron units) an atom uses for bonding.
	Bond critical point	The minimum in the charge density along a *bond path*.
s	Bond flux	A measure of the strength of a bond in valence units equal to the amount of charge contributed by each atom to form the bond, also known as the bond valence.
R_{MO}	Bond length	The distance between a cation M and oxygen.
	Bond path	The path of steepest descent in the charge density linking two neighbouring nuclei.
r	Bonded radius.	The distance between the atomic nucleus and the *bond critical point*.
S	Bonding strength.	The valence of a typical bond equal to the *atomic valence* divided by the *typical coordination number* (Eq. 5).
	QTAIM	Quantum theory of atoms in molecules [1].
f	Fractional bonded radius	(Equations 18, 19).
n	Row number	In the periodic table, the rows are numbered with the H and He row as zero. The row number is equal to the number of quantum shells in the atom core.
N	Coordination number	The number of bonds formed by an atom
$<N>$	Typical coordination number	The average observed *coordination number* (Eq. 5).
S	Typical bond flux	See bonding strength.
R_S	Typical bond length	The length of a bond with a flux equal to the cation *bonding strength* (Eq. 16).
r_S	Typical bonded radius	The radius of an atom when forming a bond with a flux equal to its *bonding strength* (Eq. 21)
R_n, R_1	Univalent bond length	Length of the M-O bond with a *bonding strength* 1.0 vu where M is in the *n*th (or first) row of the periodic table (Eqs. 12, 15).
r_0	Univalent bonded radius	Typical bonded radius that an atom would have if its *bonding strength* were 1 vu.
vu	Valence unit	Unit of charge or flux, equal to one electron unit.

Compliance with ethical standards

Conflict of interest The author has no conflicts of interest.

Funding This work was not supported by any funding.

References

1. Bader RWF (1990) Atoms in molecules: a quantum theory. Clarendon Press, Oxford
2. Bader RWF (2009) Bond paths are not chemical bonds. J Phys Chem A 113:10391–10396
3. Brown ID (2016) The chemical bond in inorganic chemistry: the bond valence model, 2nd edn. Oxford University Press, Oxford
4. Preiser C, Lösel J, Brown ID, Kunz M, Skowron A (1999) Long range forces and localized bonds. Acta Cryst B55:698–711
5. Brown ID (2016) Bond valence parameters. http://www.iucr.org/resources/data/datasets/bond-valence-parameters. Accessed 2016–2-1
6. Boison MB, Gibbs GV, Zhang JG (1988) Resonant bond numbers: a graph theoretic study of bond length variation is silicate crystals. Phys Chem Minerals 15:409–415
7. Downs RT, Gibbs GV, Boison Jr MB, Rosso KM (2002) A comparison of procrystal and ab initio model representations of the electron-density distributions of minerals. Phys Chem Minerals 29:369–385
8. Gibbs GV, Ross NL, Cox DF, Rosso KM (2014) Insights into the crystal chemistry of earth materials rendered by electron density distributions: Pauling's rules revisited. Amer Min 99:1071–1084
9. Shannon RD, Prewitt CT (1969) Effective ionic radii in oxides and fluorides. Acta Cryst B25:925–946
10. Gibbs GV, Boison Jr MB, Beverly LL, Rosso KM (2001) A computational quantum chemical study of the bonded interactions in earth materials and structurally and chemically related molecules. In: Cygan RT, Kubicki JD (eds) Molecular modelling theory: applications in the geosciences, vol 42. Mineralogical Society of America, Chantilly, pp. 345–381 . doi:10.2138/rmg.2001.42.10**Reviews in Minerology**
11. Brown ID, Shannon RD (1973) Empirical bond-strength bond length curves for oxides. Acta Cryst A29:266–282
12. Brown ID (1988) What factors determine cation coordination numbers. Acta Cryst B44:545–553
13. Belsky A, Hellenbrandt M, Karen VL, Luksch P (2002) New developments in the inorganic crystal structure Database (ICSD): accessibiltiy in support of materials research and design. Acta Cryst B58:364–369
14. Bickmore BR, Wander MFC, Edwards J, Maurer J, Shepherd K, Meyer E, Johansen WJ, Frank RA, Andros C, Davis M (2013) Electronic structure effects in the vectorial-bond-valence model. Amer Min 98:340–349
15. Gillepie RJ, Hargittai I (2012) The VSEPR model of molecular geometry. Dover, New York
16. Gillespie RJ, Popelier PLA. (2001) Chemical bonding and molecular geometry Allyn and Bacon, Boston
17. Hirschfeld FL, Rzotkiewicz S (1974) Electrostatic binding in the first-row AH and A2 diatomic molecules. Mol Phys 27:1319–1343
18. Sanderson RT (1983) Polar covalence. Academic Press Inc., New York